# Roughness effects on the thermal stability of thin films

Palasantzas, George

# Roughness effects on the thermal stability of thin films

George Palasantzas[a)]

*Delft University of Technology, Department of Applied Physics, Lorentzweg 1, 2628 CJ Delft, The Netherlands*

In this work, we investigate interface roughness effects on the energetic terms that play a key role on the thermal stability of thin silicide films. The roughness is modeled as a self-affine structure with power spectrum $\sim \sigma^2 \xi^2 (1 + aq^2\xi^2)^{-1-H}$ convoluted with a domain size distribution $\propto e^{-\pi R^2/\zeta^2}$ to account for grain finite size effects in polycrystalline films. The parameters $\sigma$, $\xi$, $H$, and $\zeta$ denote respectively the rms roughness, the roughness correlation length, the roughness exponent, and the average domain size. The roughness effect becomes significant for small $H$ ($<0.5$), and large long-wavelength roughness or $\sigma/\xi (\sim 0.1)$. Indeed, in systems where agglomeration occurs via thermal grooving, roughness may increase significantly the critical grain sizes. © *1997 American Institute of Physics.* [S0021-8979(97)00901-8]

## I. INTRODUCTION

The application of metal silicide thin films has been more than a shining success in the field of semiconductor technology. As a result, there is an enormous interest in the fabrication of metal silicide thin films (i.e., $NiSi_2$, $CoSi_2$, $TiSi_2$)[1] due to their application in complementary-metal-oxide-semiconductor processes (CMOS),[2] and microelectronics circuits (gates, contacts, interconnects, etc.)[3] Moreover, their low resistivity makes them important for the formation of self-aligned silicides[4] in ultralarge-scale integrated (ULSI) devices where deep submicron ($<300$ nm) design rules are required.

However, in many cases the application of silicides in microelectronics is limited by stability problems at high temperatures since agglomeration of the film into discrete islands occurs. A variety of degradation mechanisms which deal with grain size, grain-boundary energy, and silicide interface and surface energy have been proposed.[5] It is suggested that small grain size, small grain-boundary energy, large surface/interface energy, or thicker films may result in better thermal stability.[5,6] Indeed, the surface energy in metals is much larger than grain-boundary and interface energy.[7] If metal silicides pertain to the same property,[6] a large surface energy suggests that it is more possible that thermal grooving starts at the silicide/Si interface rather than at the silicide surface. As a result an increment in the silicide surface energy is not as efficient as an increment in the silicide/Si interface energy to prevent film agglomeration.[6,8] Therefore, the interface energy will be the key factor which determines the thermal stability of the films.

The silicide/Si interface can be rough as a result of various physical processes that are related to silicide thermal stability and/or growth process. Indeed, a thin film could release its high surface energy through Si precipitation and silicide/Si interface roughness.[6] Alternatively, the silicide growth processes could result in silicide/Si rough interfaces as for example in $CoSi_2$ formed via the nucleation control process[1,9] associated in many cases with a native oxide on the original Si surface.[9] Therefore, the silicide/Si interface can be rough and this roughness contributes positively to the interfacial energy, and thus to resistance against agglomeration to a degree that depends on the specific local and global roughness characteristics. The interface roughness will be modeled as self-affine fractal since it has been observed in many physical systems of vapor deposited thin films.[10,11] Furthermore, in order to account for finite grain sizes in polycrystalline films (e.g., $TiSi_2$[5]), we will consider a distribution of domains aligned parallel to each other and with the domain terrace to possess self-affine roughness.[12] Indeed, the growth of larger area epitaxial silicides eliminates thermal grooving paths possibly promoting the silicide thermal stability.[6,13]

## II. ROUGHNESS CONTRIBUTION TO SURFACE/INTERFACE ENERGY

We denote the surface/interface height profile by $h(r)$ which is assumed a single valued random function of the in-plane position vector $r=(x,y)$. The energy of a rough interface is given by $F_r = \int \gamma [1+(\nabla h)^2]^{1/2} d^2r$ with $\gamma$ the surface/interface free energy. For isotropic roughness in $x-y$ directions, we may assume that $\gamma$ is isotropic and as a result can be factored out of the integral of $F_r$. For weak roughness or $|\nabla h| \ll 1$, $[1+(\nabla h)^2]^{1/2} \approx 1+(1/2)(\nabla h)^2 - (1/8)(\nabla h)^4 \cdots$ which upon substitution into $F_r$ yields

$$F_r \approx F_{\text{flat}} + \gamma \left( \frac{1}{2} \int (\nabla h)^2 d^2r - \frac{1}{8} \int (\nabla h)^4 d^2r \right), \quad (2.1)$$

where $F_{\text{flat}} = \gamma A_{\text{flat}}$, with $A_{\text{flat}} \approx \int d^2r$ the macroscopic average flat area (for which $\langle h(r) \rangle = 0$). In the strong roughness limit or $|\nabla h| \gg 1$, $[1+(\nabla h)^2]^{1/2} \approx |\nabla h| + (1/2)|\nabla h|^{-1}$ which upon substitution into $F_r$ yields

$$F_r \approx \gamma \left( \int |\nabla h| d^2r + \frac{1}{2} \int |\nabla h|^{-1} d^2r \right). \quad (2.2)$$

From Eqs. (2.1) and (2.2) we can define an effective surface/interface energy $F_r/A_{\text{flat}}$ that incorporates corrections due to roughness.
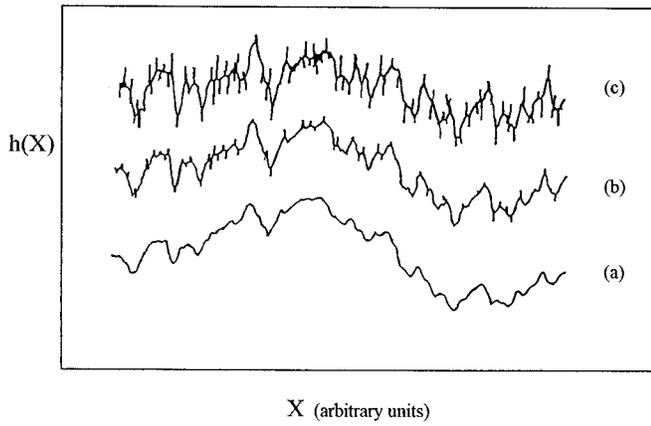
FIG. 1. Schematics of the height profile $h(X)$ vs the in-plane position $X$ for self-affine structures in order to show the effect of the roughness exponent $H$ (see Refs. 6 and 8): (a) $H=0.8$, (b) $H=0.5$, (c) $H=0.2$.

## III. ROUGHNESS MODELING

A wide variety of surfaces and interfaces occurring in nature are well represented by a kind of roughness associated with self-affine fractal scaling, defined by Mandelbrot in terms of fractional Brownian motion.[11] Examples include the nanometer topology of vapor-deposited thin films, the spatial fluctuations of liquid–gas interfaces, the kilometer-scale structure of mountain terrain, etc.[10,11] Physical processes which produce such surfaces include fracture, erosion, molecular beam epitaxy (MBE), fluid invasion in porous media, etc.[10,11]

The correlation function $C(r)=\langle h(r)h(0)\rangle$ for any physical isotropic self-affine surface scales as $C(r) \approx \sigma^2 - Dr^{2H}$ for $r \ll \xi$, and $C(r)=0$ for $r \gg \xi$ ($D \sim \sigma^2/\xi^{2H}$ is a constant).[10,11,14–16] $\sigma^2 = \langle h(r)^2 \rangle$ is the mean-square departure of the surface from flatness (rms surface roughness). The correlation length $\xi$ represents the average distance between consecutive peaks or valleys on the surface. The roughness exponent $0 < H < 1$ is a measure of the degree of surface irregularity.[10,15] Small values of $H(\sim 0)$ characterize extremely jagged or irregular surfaces, while large values $H(\sim 1)$ surfaces with smooth hills and valleys, Fig. 1.[10,11] The Fourier transform of $C(r)$ scales as $\langle |h(q)|^2 \rangle \propto q^{-2-2H}$

if $q\xi \gg 1$, and $\langle |h(q)|^2 \rangle \propto$ const if $q\xi \ll 1$.[10,11] Such a scaling behavior is satisfied by the *k-correlation model*,[16]

$$\langle |h(q)|^2 \rangle = \frac{A_{\text{flat}}}{(2\pi)^5} \frac{\sigma^2 \xi^2}{(1+aq^2\xi^2)^{1+H}}, \tag{3.1}$$

which is valid for the whole range of values for the roughness exponent $0 \leq H < 1$. The parameter "$a$" is given by $a = 1/2H[1 - (1+aQ_c^2\xi^2)^{-H}]$ if $0 < H < 1$, and $a = 1/2 \ln(1+aQ_c^2\xi^2)$ if $H=0$. $Q_c = \pi/a_0$ with $a_0$ the atomic spacing. The logarithmic roughness for $H=0$ is related to predictions of growth models of the nonequilibrium analogue of the equilibrium roughening transition.[17] The value $H=1$ is related to the formation of large mountain-valley structures, and has been observed in films grown in an epitaxial fashion associated with growth instabilities during film evolution.[10,14,18]

Furthermore, we consider the more complex surface structure of domains aligned parallel to each other and with domain terrace to possess self-affine roughness in order to model polycrystalline films with finite size grains. The effect of domains sizes and shapes can be simulated through a radial Gaussian distribution function $\propto e^{-\pi R^2/\zeta^2}$[12,19] with $\zeta$ the average domain size, and roughness spectrum $\langle |h(q)|^2 \rangle_d$ which reads of the form[12]

$$\langle |h(q)|^2 \rangle_d$$

$$\approx \begin{cases} [A_{\text{flat}}/(2\pi)^6]\sigma^2\zeta^2 e^{-q^2\zeta^2/4\pi}, & \zeta \ll \xi \\ \langle |h(q)|^2 \rangle + [A_{\text{flat}}/(2\pi)^6] \dfrac{\sigma^2\pi\xi^2\zeta^2}{\pi\xi^2+\zeta^2} e^{-q^2\zeta^2/4\pi}, & \zeta \approx \xi \\ \langle |h(q)|^2 \rangle, & \zeta \gg \xi. \end{cases} \tag{3.2}$$

## IV. RESULTS AND DISCUSSION

For both roughness limits, we can define an effective (ensemble averaged over roughness realizations) interfacial free energy or surface tension $\Gamma_e = \langle F_r \rangle/A_{\text{flat}}$ which incorporates surface/interface roughness effects. Moreover, the knowledge of the integrals $S_{1,d}(\sigma,\xi,H) = [(2\pi)^4/A_{\text{flat}}]\int_{0<q<Q_c} q^2\{\langle |h(q)|^2 \rangle, \langle |h(q)|^2 \rangle_d\}d^2q$ will be required for the calculation of $\Gamma_e$. In fact, substituting from Eqs. (3.1) to (3.2) we obtain

$$S_1(\sigma,\xi,H) = \begin{cases} \dfrac{\sigma^2}{2a^2\xi^2} \left\{ \dfrac{1}{1-H}[(1+aQ_c^2\xi^2)^{1-H}-1]-2a \right\} & (0 \leq H < 1) \\ \dfrac{\sigma^2}{2a^2\xi^2} \{\ln(1+aQ_c^2\xi^2)-2a\}, & (H=1). \end{cases}$$

$$S_d(\sigma,\xi,H,\zeta) \approx S_1(\sigma,\xi,H) + \frac{4\pi^2\sigma^2\xi^2}{\zeta^2(\pi\xi^2+\zeta^2)}$$
$$\times \{1 - e^{-Q_c^2\zeta^2/4\pi} - (Q_c^2\zeta^2/4\pi)e^{-Q_c^2\zeta^2/4\pi}\}, \tag{4.1}$$

where the limit $H=1$ is obtained from the identity $\lim_{a\to 0}(1/a)(x^a-1)=\ln(x)$. The bottom inset of Fig. 2 displays $S_{1,d}(\sigma,\xi,H)$ vs $H$.

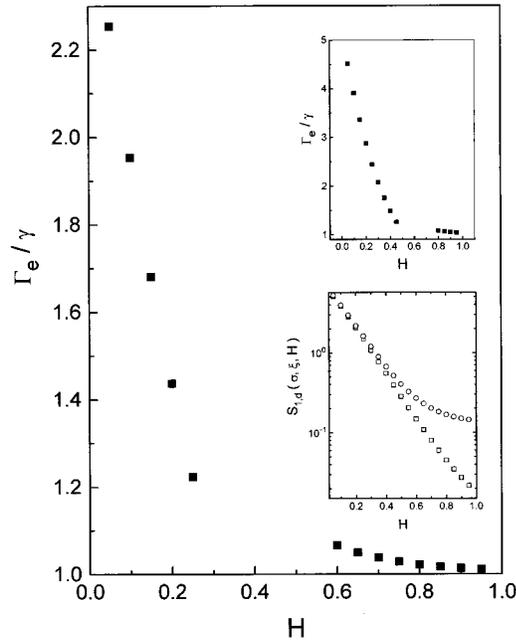In the weak roughness limit Eq. (2.1) [Appendix, Eq. (A2)] yields

FIG. 2. Schematics of $\Gamma_e/\gamma$ vs the roughness exponent $H$ in terms of Eqs. (4.2) and (4.3). $\zeta=3\xi$ (finite domains), $\sigma/\xi=0.03$, $\xi=30$ nm, $a_0=0.3$ nm. The top inset depicts the same calculation but with ratio $\sigma/\xi=0.06$. The bottom inset depicts $S_{1,d}(\sigma,\xi,H)$ vs $H$ with $\sigma/\xi=0.03$, $\xi=30$ nm, $a_0=0.3$ nm. Squares represent the case of no domains or $\zeta\gg\xi$, and the circles finite domains with $\zeta=0.3\xi$.



FIG. 3. Schematics of $\Gamma_e/\gamma$ vs the roughness exponent $H$ in terms of Eqs. (4.2) and (4.3). $\sigma/\xi=0.03$, $\xi=30$ nm, $a_0=0.3$ nm, squares: $\zeta=+\infty$ (no domains); upper-triangles: $\zeta=3\xi$ (finite size domains). The inset shows the same calculation but with domain finite size $\zeta=0.3\xi$.

$$\Gamma_{e1,d}\approx\gamma\left\{1+\tfrac{1}{2}S_{1,d}(\sigma,\xi,H)-\tfrac{3}{8}[S_{1,d}(\sigma,\xi,H)]^2\right\} \quad (4.2)$$

by proper Fourier transformation of the terms $(\nabla h)^{2n}$ ($n=1,2$) and grouping of the integrated ensemble-averaged products with $2n$ terms. However, in the strong roughness limit we can calculate mainly an upper limit for the interface energy. In fact, the inequality $\langle|\nabla h|\rangle\leqslant\langle|\nabla h|^2\rangle^{1/2}$ yields after substitution in Eq. (2.2) to the lowest order $\langle F_r\rangle/F_{\text{flat}}\approx\int\langle|\nabla h|\rangle d^2r\leqslant\int[\langle|\nabla h|^2\rangle]^{1/2}d^2r$. Fourier transforming and taking into account Eq. (4.1) we obtain

$$\Gamma_{e1,d}\leqslant\gamma[S_{1,d}(\sigma,\xi,H)]^{1/2}, \quad (4.3)$$

which represents an upper bound for the roughness contribution to first order of approximation.

Prior to the presentation of the results, we point out the following. The ratio $\sigma/\xi$ describes mainly the long-wavelength ($q\ll1/\xi$) roughness characteristics. Finer roughness details at short wavelengths ($q\gg1/\xi,1/\zeta$) are revealed through the effect of the roughness exponent $H$, which describes the degree of height–height fluctuation density and it is related with a local interface/surface fractal dimension $D=3-H$.[10,11,15] In our calculations, we used the correlation length $\xi=30.0$ nm, values for $\sigma$ such that $\sigma/\xi\leqslant0.1$, domain sizes in the range $\zeta\sim(0.3-3)\xi$, and roughness exponents in the range $0\leqslant H<1$. The chosen values for the parameters $\sigma$, $\xi$, $\zeta$, and $H$ are based on a wide variety of experimental roughness studies,[10,13] and agglomeration studies of silicides films where grain sizes of the order of $\sim50$ nm or larger (e.g., $TiSi_2$, $CoSi_2$)[5,6] were observed.

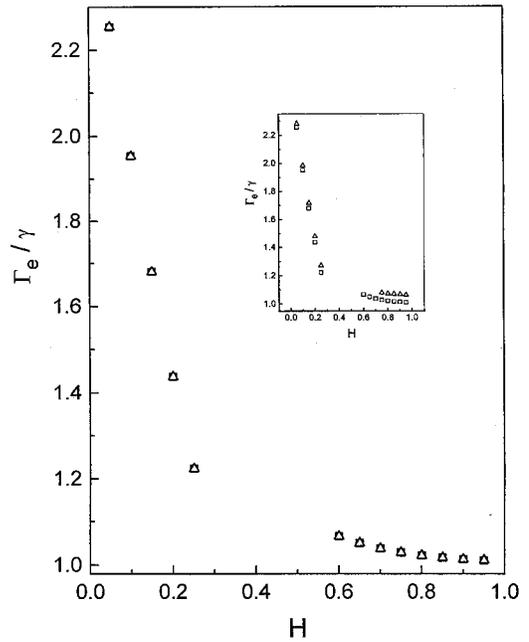In Figs. 2 and 3, we plot simultaneously the weak roughness limit [Eq. (4.2)] with the upper bound strong roughness limit [Eq. (4.3)] of $\Gamma_e$ vs $H$ and ratios $\sigma/\xi$ in the range $0.03\leqslant\sigma/\xi\leqslant0.06$. In all schematics, there is a discontinuity of $\Gamma_e$ as a function of $H$ signifies the crossover from the strong to weak roughness limit regime. It is observed that as the ratio $\sigma/\xi$ increases the crossover occurs at larger roughness exponents $H$. More precisely, from Fig. 2 we obtain a crossover at $H>0.3$ for $\sigma/\xi=0.03$, and for $\sigma/\xi=0.06$ at $H>0.5$. The effect of the average domain size $\zeta$ on $\Gamma_e$ is rather negligible for $\zeta>\xi$ to the order of $(\sigma/\xi)(\xi^2/\zeta^2)$ since $Q_c\zeta\gg1$ [Eq. (4.1), Fig. 3]. However, for $\zeta<\xi$ (the inset of Fig. 3) it becomes significant for large $H(>0.5)$ influencing also the crossover to weak roughness limit which occurs at larger $H$ as $\zeta$ decreases below $\xi$.

From Fig. 2, it is observed that the upper bound of the interface energy (strong roughness limit or $S_{1,d}>1$) could be significantly larger (depending on the roughness parameters) than the energy $\gamma$ of a flat area. This occurs mainly at large ratios $\sigma/\xi\sim0.1$, and small roughness exponents $H$. The latter is in agreement with the fact that as $H$ becomes small ($H<0.5$), the number of surface crevices increases (see Fig. 1) therefore exposing a larger area which leads effectively to higher surface energies ($\Gamma_e>\gamma$). Moreover, from Fig. 2 we can see that the dominant effect comes from the ratio $\sigma/\xi$. In fact from Eqs. (4.1) and (4.3), the upper bound of the effective interface energy is directly proportional to $\sigma/\xi$; $\Gamma_e/\gamma\propto\sigma/\xi$ (assuming $\zeta\approx\xi$). Nevertheless, the increment at small $H$ ($<0.5$) appears to be characteristically steep as a function of the roughness exponent $H$.

*Critical grain size:* Since surface/interface roughness could have a significant contribution on the thin film key parameters that determine its thermal stability, we will examine qualitatively the roughness contribution in polycrystalline films where the agglomeration mechanism can be thermal grooving at grain boundaries. In fact, Nolan *et al.*[5]
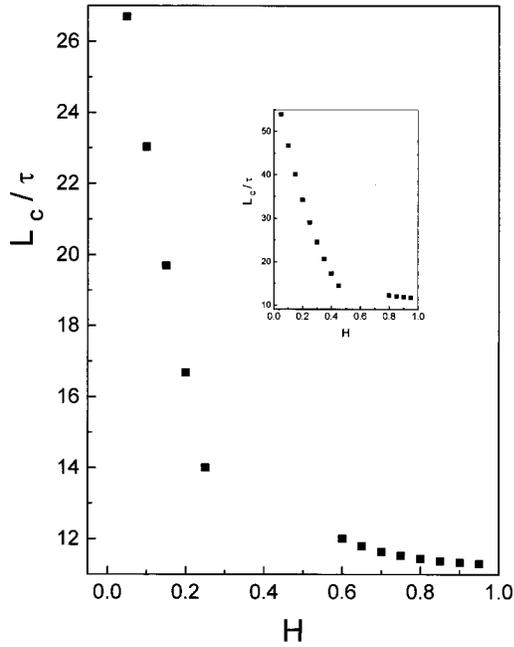
FIG. 4. Schematics of $L_c/\tau$ vs the roughness exponent $H$. $\zeta = 3\xi$, $\sigma/\xi = 0.03$, $\xi = 30$ nm, $a_0 = 0.3$ nm. The inset shows the same calculation but with ratio $\sigma/\xi = 0.06$.

calculated the maximum grain size $L_c$ for which agglomeration cannot occur via this mechanism. If we define by $\gamma_i, \gamma_s, \gamma_b$, respectively, the interface, surface, and grain boundary energies, the critical grain size $L_c$ is given by $L_c\tau = 2/[f(\theta_i) + f(\theta_s)]$[15] with $\tau$ the film thickness, $\theta_{i,s} = \sin^{-1}(\gamma_b/2\gamma_{i,s})$ and $f(\theta) = \{[(2+\cos^3\theta)/3] - \cos\theta\}/\sin^3\theta$. For comparable grain boundary and interface energies and about 1/3 of the surface free energy ($\gamma_b \approx \gamma_i \approx \gamma_s/3$; pure metals[5,7,20]), $L_c \approx 10\tau$ is obtained.[5] Agglomeration can be prevented as long as the grain size is less than $L_c$ which can be achieved if one decreases the grain size and boundary energy, and increases film thickness and surface/interface energies.

Since surface/interface roughness effectively leads to larger free energies $\Gamma_e$, by making the assumption that surface and interface possess the same roughness, $\gamma_b \approx \gamma_i \approx \gamma_s/3$, and substituting $\gamma_{i,s} \rightarrow (\Gamma_e)_{i,s}$, we can estimate the roughness effect on $L_c$. Figure 4 shows calculations of $L_c$ vs $H$ where a characteristic sensitivity of $L_c$ on the roughness exponent $H$ and consequently on the surface/interface irregularity is observed. At small roughness exponents $H < 0.5$ and typically large ratios $\sigma/\xi$ ($\sim 0.1$), the ratio $L_c/\tau$ can be increased significantly from that for smooth surfaces/interfaces ($L_c \approx 10\tau$). In the limit of strong roughness or $S \gg 1$ [Eqs. (4.1) and (4.3)] and for surface/interface energies such that $\gamma_{i,s} \cong \gamma_b$ (or $\gamma_{i,s} > \gamma_b$), we obtain $f(\theta_{i,s}) \approx (\gamma_b/2\gamma_{i,s})/(4S_{1,d})$ (see the Appendix) which finally yields

$$L_c/\tau \approx 8\left[\left(\frac{\gamma_b}{2\gamma_i}\right)\frac{1}{S_{1,d}^i} + \left(\frac{\gamma_b}{2\gamma_s}\right)\frac{1}{S_{1,d}^s}\right]^{-1}. \quad (4.4)$$

For large roughness exponents $H$ ($\sim 1$) or smoother structures, the ratio $L_c/\tau$ attains values such that $L_c \approx 10\tau$ in agreement with the prediction where roughness was not included.[5]

Therefore, despite the simplifying assumptions, our qualitative estimate of the roughness effects on $L_c$ indicates that surface/interface roughness has to be taken seriously into account in thin film degradation mechanisms.

## V. CONCLUSIONS

In conclusion, we combined knowledge of basic thin film thermal stability theories with that of analytic height–height correlation models for self-affine fractals, in order to investigate quantitatively and qualitatively the surface/interface roughness effect on degradation processes which involves agglomeration into discrete islands. Our results shows clearly that this effect becomes of significant quantitative importance for interfaces/surfaces with large ratios $\sigma/\xi(\sim 0.1)$, and small roughness exponents $H(<0.5)$ (strong roughness limit). More precisely, estimations of the strong roughness limit shows that the corresponding surface/interface energies can be of the order of $\Gamma_e \sim 5\gamma$ or even more. Indeed, application to simple theoretical models which apply to the case of polycrystalline thin films (modeled as domains with a Gaussian size distribution), shows that the contribution of surface/interface roughness has a strong impact on critical grain sizes below which the film still pertains its continuous structure.

Therefore, surface/interface roughness effects have to be considered seriously in future precise modeling of degradation mechanisms. Moreover, extensive studies will be required on each particular thin-film structure to gauge precisely the roughness contribution in connection with the film fabrication conditions and system temperature as long as the thermal stability of the particular system is concerned.

## APPENDIX

### 1. Surface/interface energy

In the weak roughness limit, the ensemble averaged full expansion of Eq. (2.1) is given by

$$\langle F_r \rangle = F_{\text{flat}} + \gamma \sum_{n=1}^{+\infty} \{(1/2)(1/2-1)\cdots(1/2-n+1)/n!\}$$

$$\times \int \langle(\nabla h)^{2n}\rangle d^2r. \quad (A1)$$

Moreover, if we assume the interface height ''$h$'' to be a Gaussian variable, then the average of any odd number of factors of $h$ with the same or different arguments vanishes, whereas the average of the product of an even number is given by the sum of the products of the averages of $h$'s paired two-by-two in all possible ways.[21] Thus, as was shown in earlier studies,[22] we have

$$\langle (\nabla h)^{2n} \rangle = i^{2n} \int \left\langle \prod_{j=1}^{2n} h(q_j) \right\rangle \left( \prod_{j=1}^{2n} q_j \right)$$

$$\times \exp\left[ -i\left( \sum_{j=1}^{2n} qj \right) r \right] \prod_{j=1}^{2n} d^2 q_j$$

$$= P(n)[S_{1,d}(\sigma, \xi, H)]^{2n}$$

with $P(1)=1$ and $P(2)=3$. Further concepts of statistics are needed to calculate $P(n>2)$ which represents all possible ways to group $2n - h(q)$'s ensemble averaged in pairs of two.[21,23] Moreover, Eq. (A1) takes the form

$$\langle F_r \rangle = F_{\text{flat}} \left\{ 1 + \sum_{n=1}^{+\infty} \{(1/2)(1/2-1)\cdots(1/2-n+1)/n!\} \right.$$

$$\left. \times P(n)[S_{1,d}(\sigma, \xi, H)]^n \right\}. \tag{A2}$$

## 2. Grain size

The expansion up to second order of the terms $\cos \theta_{i,s}$ (strong roughness limit) in $f(\theta_{i,s}) = \{[(2+\cos^3 \theta_{i,s})/3] - \cos \theta_{i,s}\}/\sin^3 \theta_{i,s}$ (Ref. 5) reads of the form

$$\cos^{2b} \theta_{i,s} \approx 1 - b\left( \frac{\gamma_b}{2\gamma_{i,s}} \right)^2 (S_{1,d}^{i,s})^{-2}$$

$$+ \frac{b(b-1)}{2} \left( \frac{\gamma_b}{2\gamma_{i,s}} \right)^4 (S_{1,d}^{i,s})^{-4} \tag{A3}$$

with $b = 1/2, 1/3$. Substitution into the expression for $f(\theta_{i,s})$ leads finally to Eq. (4.4) in a straightforward manner.

[1] R. T. Tung, Met. Chem. Phys. **32**, 107 (1992); H. von Kanel et al., Appl. Surf. Sci. **53**, 196 (1991).

[2] Y. Yamaguchi et al., IEEE Trans. Electron Devices **ED-39**, 1179 (1992); H. Ronkainen et al., ibid. **EDL-12**, 125 (1991); S. Parekh et al., ibid. **ED-38**, 88 (1991).

[3] R. T Tung and F. Schrey, Appl. Phys. Lett. **67**, 2164 (1995).

[4] K. Maex, Mater. Sci. Eng. R. Rep. **11**, 53 (1993).

[5] T. P. Nolan et al., J. Appl. Phys. **71**, 720 (1992); Z. G. Xiao et al., Mater. Res. Soc. Symp. Proc. **202**, 101 (1991).

[6] B.-S. Chen and M.-S. Chen, J. Appl. Phys. **74**, 1035 (1993).

[7] L. E. Murr, Interfacial Phenomena in Metals and Alloys (Addison-Wesley, Reading, MA, 1975), pp. 122–135.

[8] B. Y. Tsui et al., IEEE Trans. Electron Devices **ED-40**, 54 (1993); T. P. Nolan et al., J. Appl. Phys. **71**, 720 (1992).

[9] F. M. D.'heurle and C. S. Peterson Thin Solid Films **128**, 283 (1985).

[10] P. Meakin, Phys. Rep. **235**, 1991 (1994); J. Krim and G. Palasantzas, Int. J. Mod. Phys. B **9**, 599 (1995) (Schematics similar to Fig. 1 in this work which show the effect of $H$, can also be found in Fig. 1 of this reference).

[11] B. B. Mandelbrodt, The Fractal Geometry of Nature (Freeman, New York, 1982); F. Family and T. Viscek, Dynamics of Fractal Surfaces (World Scientific, Singapore, 1991). The schematics of Fig. 1 show only the effect of the roughness exponent $H$ without including any particular $\sigma$ and $\xi$, and can be produced by computer graphic algorithms: see R. F. Voss, in Fundamental Algorithms for Computer Graphics, edited by R. A. Earshaw (Springer, Berlin, 1985), p. 808; R. F. Voss, in Scaling Phenomena in Disordered Systems, edited by R. Pynn and A. Skjeltrop (Plenum, New York, 1985), p. 1.

[12] G. Palasantzas, Phys. Rev. B **49**, 10544 (1994).

[13] The epitaxial argument is still under investigation, since scanning electron microscopy (SEM) observations indicated a uniform retardation of film agglomeration (see also Ref. 6).

[14] G. Palasantzas and J. Krim, Phys. Rev. Lett. **73**, 3564 (1994).

[15] G. Palasantzas, Phys. Rev. E **49**, 1740 (1994); J Krim and J.O. Indekeu, ibid. **48**, 1576 (1993).

[16] G. Palasantzas, Phys. Rev. B **48**, 14472 (1993); **49**, 5785(E) (1994).

[17] G Amar et al., Phys. Rev. Lett. **64**, 542 (1990); J. Krug et al., ibid. **64**, 2332 (1990); J. M. Kim et al., ibid. **64**, 2333 (1990); D. A. Huse et al., Phys. Rev. B **41**, 7075 (1990); J. Villain et al., J. Phys. F **15**, 805 (1985); J. Jose et al., Phys. Rev. B **16**, 1217 (1977).

[18] M. Siegert and M. Plischke, Phys. Rev. Lett. **73**, 1517 (1994).

[19] P. Dutta and S. K. Sinha, Phys. Rev. Lett. **47**, 50 (1981).

[20] H. Jones, Met. Sci. J. **5**, 15 (1971).

[21] G. A. Farias and A. A. Maradudin, Phys. Rev. B **28**, 5675 (1983). See page 5676 for these basic concepts of random rough surfaces.

[22] G. Palasantzas and E. Koumanakos, J. Appl. Phys. **79**, 8531 (1996).

[23] M. R. Spiegel, Probability and Statistics, Schaum's Outline Series (McGraw-Hill, New York, 1975).